ESAIM: M2AN 46 (2012) 1389–1405
DOI: 10.1051/m2an/2012007

ESAIM: Mathematical Modelling and Numerical Analysis
www.esaim-m2an.org

COMBINED *A POSTERIORI* MODELING-DISCRETIZATION ERROR ESTIMATE FOR ELLIPTIC PROBLEMS WITH COMPLICATED INTERFACES

Sergey I. Repin[1], Tatiana S. Samrowski[2] and Stéfan A. Sauter[2]

Abstract. We consider linear elliptic problems with variable coefficients, which may sharply change values and have a complex behavior in the domain. For these problems, a new combined discretization-modeling strategy is suggested and studied. It uses a sequence of simplified models, approximating the original one with increasing accuracy. Boundary value problems generated by these simplified models are solved numerically, and the approximation and modeling errors are estimated by *a posteriori* estimates of functional type. An efficient numerical strategy is based upon balancing the modeling and discretization errors, which provides an economical way of finding an approximate solution with an a priori given accuracy. Numerical tests demonstrate the reliability and efficiency of this combined modeling-discretization method.

Mathematics Subject Classification. 35J15, 65N15, 65N30.

Received October 27, 2010. Revised April 7, 2011.
Published online April 11, 2012.

1. Introduction

We consider elliptic boundary value problems with rather complex behavior of the coefficients. As a model problem we choose the diffusion equation $\operatorname{div}(A \operatorname{grad} u) = f$ in a two- or three-dimensional bounded domain with homogeneous Dirichlet boundary conditions. From the physical point of view, this equation can be regarded as a model of a stationary diffusion. Our focus is on diffusion matrices A which are piecewise smooth but allow for discontinuities along interfaces with, possibly, very rough and complicated structure.

Certainly, there is a straightforward way to solve such problems which consists of solving numerically the problem on a sufficiently fine mesh which resolves all geometric scales of the interfaces and eliminates the quadrature errors arising from the generation of the stiffness matrix. In particular for three-dimensional problems with rough interfaces this approach could by far exceed the capacity of modern computers. If solely a numerical solution with a moderate guaranteed accuracy is required, the following strategy, typically, is preferable. It consists of two basic steps. First, complicated interfaces which are separating the regions of smoothness of the diffusion matrix are replaced by a simpler one and a new diffusion matrix is set up on the simplified regions by some averaging technique. This simplified model is discretized and numerically solved on a rather coarse mesh which only has to resolve the simplified regions. In the second step, the discretization and modeling errors are

Keywords and phrases. A posteriori error estimate, complicated diffusion coefficient, defeaturing of models, combined modeling discretization adaptive strategy.

[1] V.A. Steklov Institute of Mathematics, Russian Academy of Sciences, Fontanka 27, 191023 St. Petersburg, Russia. repin@pdmi.ras.ru

[2] Institut für Mathematik, Universität Zürich, 8057 Zürich, Switzerland. tatiana.samrowski@math.uzh.ch; stas@math.uzh.ch

controlled with the help of *a posteriori* estimates. A guaranteed upper bound of the total error is determined as the sum of discretization and modeling errors, which are both explicit and computable. If the bound exceeds the given tolerance, then either the mesh should be refined (if the discretization error dominates) or the coefficient behavior must be modeled more accurately (if the modeling error dominates). Hence, the solution process is a *combined modeling-discretization* strategy for balancing the modeling error E_{mod} and the discretization error E_{disc} in an problem-*adapted* way.

Historically, the subject of *a posteriori* error estimation was mainly focused on the indication of discretization errors (*e.g.*, see [3,33], and references therein). In these cases, the error is measured by the quantity $\|u - u_h\|$, where u is the exact solution, u_h is the Galerkin approximation, and $\|\cdot\|$ is a certain norm associated with the problem (see, *e.g.*, [2–6,12,15,32,33]).

Our method differs from these approaches and its derivation is based on our previous publications (see [19–31]), in which estimates of the difference between the exact solution of boundary value problems and arbitrary functions from the corresponding energy space has been derived by purely functional methods without requiring specific information on the approximating subspace and the numerical method used. As a result, the estimates contain no mesh dependent constants and are valid for any conforming approximation from the respective energy space. In the papers [30,31], these properties have been used for the analysis of modeling errors.

Also, we refer to [17], where a closely related approach has been presented. An approach, which is based on the Prager-Synge hypercircle method, is presented in [10,11]. Also there, mesh dependent constants can be avoided in the *a posteriori* error estimates. This approach is elegant when applied to certain non-conforming finite element discretizations. On the other hand, it is limited to the complementary energy principle. In contrast our approach is also applicable to problems that have no variational (primal/dual) energy formulation (see [21–23]). Explicit and computable estimates of modeling errors related to dimension reduction models of diffusion type problems have been derived in [28,29]. For more complicated plate models in the theory of linear elasticity, such type estimates have been recently derived in [24]. The problem of hierarchical modeling and dimension reduction has also been investigated in [7,32,35].

The present paper is concerned with modeling errors of a different nature that arises due to simplification of the interfaces and, in turn, of the coefficients. Our focus is on problems which have very complicated and irregular interfaces separating the smooth regions of the diffusion matrix and, in general, cannot be solved efficiently within the framework of homogenization theory because (a) we allow for non-periodic diffusion coefficient and (b) allow in periodic cases that the number of "cells" (allowing again for complicated cell boundaries) is too small that the approximation by a homogenized model does not lead to a satisfactory accuracy.

The structure of the paper is as follows. In Section 2, we present an adaptive, combined modeling-discretization estimation strategy for a class of elliptic boundary value problems with variable coefficients. It is based upon guaranteed upper bounds of the discretization and modeling errors, generated by simplified elliptic problems. Section 3 is devoted to a detailed description of the corresponding error control procedure. In Section 4, results of numerical tests are presented and discussed.

2. *A POSTERIORI* ERROR ESTIMATION FOR THE MODELING AND DISCRETIZATION ERROR

2.1. Setting

We consider the elliptic problem

$$\begin{aligned} -\mathrm{div}\,(A\,\nabla u) &= f \quad \text{in } \Omega, \\ u &= 0 \quad \text{on } \partial\Omega, \end{aligned} \tag{2.1}$$

where Ω is a bounded domain in $\mathbb{R}^d$ $(d = 2, 3)$ with Lipschitz boundary $\partial\Omega$, $A(x)$ belongs to the set $\mathbb{R}^{d\times d}$ of $d \times d$ matrices with real coefficients. We assume that

$$A \text{ is symmetric}, \quad A(x) \in L^\infty(\Omega, \mathbb{R}^{d\times d}), \quad f \in L^2(\Omega),$$

and

$$c_1^2\,|\zeta|^2 \;\le\; A(x)\,\zeta\cdot\zeta \;\le\; c_2^2\,|\zeta|^2 \quad \text{for all } \zeta\in\mathbb{R}^d \quad \text{and } x\in\Omega \text{ a.e.}, \tag{2.2}$$

for some positive constants c_1, c_2. Henceforth, the norm in $L^2(\Omega)$ is denoted by $\|u\|_\Omega$ and "$\cdot$" stands for the Euclidean scalar product of vectors. The notation $L^2(\Omega,\mathbb{R}^d)$ is used for the vector-valued functions with components in $L^2(\Omega)$. Let $M(x)\in\mathbb{R}^{d\times d}$. By

$$\rho(M) := \operatorname*{ess\,sup}_{x\in\Omega} \max\{|\lambda(x)| : \lambda(x) \text{ is an eigenvalue of } M(x)\} \tag{2.3}$$

we denote the supremum of the spectral radii. V_0 denotes the subspace of H^1- functions vanishing on $\partial\Omega$. Also we use the space

$$H(\Omega,\mathrm{div}) := \{q\in L^2(\Omega,\mathbb{R}^d)\,|\,\mathrm{div}\,q\in L^2(\Omega)\},$$

which is a Hilbert space endowed with the scalar product

$$(p,\,q)_{\mathrm{div}} := \int_\Omega (p\cdot q + \mathrm{div}\,p\,\mathrm{div}\,q)$$

and the norm $\|q\|_{\mathrm{div}} := (q,\,q)_{\mathrm{div}}^{1/2}$. For functions in $L^2(\Omega,\mathbb{R}^d)$, we will also need the energy and complementary energy norms

$$\|q\|_A^2 := \int_\Omega A\,q\cdot q \quad \text{and} \quad \|q\|_{A^{-1}}^2 := \int_\Omega A^{-1}\,q\cdot q. \tag{2.4}$$

The generalized solution of (2.1) is the solution of the variational problem

$$\text{Find } u\in V_0 \text{ such that} \qquad b(u,\,v) = \int_\Omega f\,v, \quad \forall v\in V_0, \tag{2.5}$$

where $b(u,\,v) := \int_\Omega A\nabla u\cdot\nabla v$ is the bilinear form generated by A. Under the above made assumptions the generalized solution exists and is unique.

In many applied models (*e.g.*, in the environmental modeling) it often happens that the coefficient $a_{ij}(x)$ has a complicated behavior. Then, the problem becomes very difficult so that solving it by standard methods often leads to a very high numerical cost. A possible way out consists of using some simplified model instead. If the modeling errors due to the simplification of data can be explicitly evaluated and proved to be essentially lower than the desired tolerance level, then this simplified model can be used instead of the original one. We show that such a simplification (defeaturing) method is indeed efficient and in many cases it is possible to obtain a solution with a practically acceptable accuracy with the help of a simplified model. For this purpose, we derive an *a posteriori* error estimate of the total error (which includes both discretization and modeling errors) and develop a solution strategy, based on the interplay between the choice of the model and the approximation subspace.

2.2. Combined modeling-discretization adaptivity

The idea of the combined *modeling-discretization adaptivity* can be explained with the help of the diagram exposed in Figure 1. Assume that the goal is to solve problem (2.1) with a guaranteed accuracy δ (measured in terms of the energy norm). This can be achieved by computing an approximate solution of the "original" problem on a sufficiently fine mesh. But the same goal can be also achieved by solving a simplified problem $\mathcal{P}_{\varepsilon_k}$ (solved on a certain finite dimensional subspace V_{h_i} ($V_{h_1}\subset V_{h_2}\ldots\subset V_{h_k}$)). The last column of Figure 1 corresponds to the usual mesh adaptivity applied to the original problem. We see that the desired accuracy is achieved for u_{h_3}. However, the cost for its numerical solution can become very large. If, for instance, the mesh does not fully

Discretization \ Model	$\mathcal{P}_{\varepsilon_1}$	$\mathcal{P}_{\varepsilon_2}$	$\mathcal{P}_{\varepsilon_3}$	...	$\mathcal{P}$
V_{h_1}	u_{ε_1,h_1}	u_{ε_2,h_1}	u_{ε_3,h_1}		u_{h_1}
V_{h_2}	u_{ε_1,h_2}	u_{ε_2,h_2}	u_{ε_3,h_2}		u_{h_2}
V_{h_3}	u_{ε_1,h_3}	u_{ε_2,h_3}	u_{ε_3,h_3}		u_{h_3}
V_{h_4}	u_{ε_1,h_4}	u_{ε_2,h_4}	u_{ε_3,h_4}		u_{h_4}
$\vdots$				$\ddots$	
V_0					u

FIGURE 1. Combined adaptive modeling-discretization strategy.

resolve the interfaces the numerical quadrature for the generation of the system matrix becomes complicated and costly. Moreover, the generation of an highly accurate resolution of zones with jumping coefficients by a finite element mesh is a difficult numerical task and requires a large number of additional nodes (elements). As a consequence the systems of linear equations (in particular, for 3D problems) becomes very large.

We consider another option. Assume that we need an approximate solution with rather moderate (engineering) accuracy. In Figure 1, the solutions having such an accuracy belong to the shaded zone.

We start the modeling-discretization adaptivity with the coarsest model $\mathcal{P}_{\varepsilon_1,h}$, and the space V_{h_1}. By the combined modeling-discretization error majorant (see Thm. 2.1), the total error associated with u_{ε_1,h_1} is estimated by the sum of the corresponding modeling error $E^{\varepsilon_1}_{\mathrm{mod}}$ and the discretization error $E^{\varepsilon_1,h_1}_{\mathrm{disc}}$. As long as the target accuracy has not been achieved (*i.e.*, the overall error exceeds the given tolerance δ) and $E^{\varepsilon_1}_{\mathrm{mod}} < \alpha\, E^{\varepsilon_1,h_1}_{\mathrm{disc}}$, where α is a positive real number that balances values of approximation and modeling errors, the subspace V_{h_1} should be refined, and we pass to V_{h_2}. If $E^{\varepsilon_1}_{\mathrm{mod}} \geq \alpha\, E^{\varepsilon_1,h_1}_{\mathrm{disc}}$, then an improved model should be chosen (we pass to $\mathcal{P}_{\varepsilon_2}$). With this strategy, an "economical" way to find a desirable approximation u_{ε_3,h_3}, is marked by arrows. It is worth mentioning that approximate solutions and their components (*e.g.*, fluxes) computed on some steps of the algorithm can further be used on subsequent steps as good initial guesses for iterative solvers.

2.3. Combined error majorant

Consider the following simplified problem $\mathcal{P}_\varepsilon$: find $u_\varepsilon \in V_0$ such that

$$b_\varepsilon(u_\varepsilon,\, v) \,:=\, \int\limits_\Omega A_\varepsilon\, \nabla u_\varepsilon \cdot \nabla v \,=\, \int\limits_\Omega f\, v \quad \text{for all } v \in V_0, \tag{2.6}$$

where $A_\varepsilon \in L^\infty(\Omega, \mathbb{R}^{d\times d})$ is a certain approximation of A. We will always assume that for any ε, the matrix A_ε is positive definite and

$$c^2_{1\varepsilon}\,|\zeta|^2 \,\leq\, A_\varepsilon(x)\,\zeta \cdot \zeta \,\leq\, c^2_{2\varepsilon}\,|\zeta|^2 \quad \text{for all } x \in \Omega \quad \text{and } \zeta \in \mathbb{R}^d. \tag{2.7}$$

Let $\mathcal{T}_h$ be a simplicial mesh with mesh size h and

$$S_h := \{u \in C^0(\overline{\Omega}) \big| \text{ for any } \tau \in \mathcal{T}_h : \mathrm{u}|_\tau \text{ is an affine function}\}.$$

Further,

$$S_{h,0} := S_h \cap V_0 \quad \text{and} \quad S_h^2 := S_h \times S_h.$$

The corresponding Galerkin solution is defined by

$$\text{Find } u_{\varepsilon,h} \in S_{h,0} \text{ such that } \quad b_\varepsilon(u_{\varepsilon,h},\, v_h) := \int\limits_\Omega A_\varepsilon\, \nabla u_{\varepsilon,h} \cdot \nabla v_h = \int\limits_\Omega f\, v_h \quad \text{for all } v_h \in S_{h,0}. \tag{2.8}$$

In order to estimate the *discretization* error $\|\nabla(u_\varepsilon - u_{\varepsilon,h})\|_{A_\varepsilon}$, we use *a posteriori* error estimates of the functional type (see [18–24, 26, 27, 30, 31] and the references therein). In our case, the estimate takes the form

$$\|\nabla(u_\varepsilon - u_{\varepsilon,h})\|^2_{A_\varepsilon} \le \mathcal{M}^2_\Omega(u_{\varepsilon,h}\,, y,\, \beta) := (1+\beta)\|A_\varepsilon\, \nabla u_{\varepsilon,h} - y\|^2_{A_\varepsilon^{-1}} + \left(1 + \frac{1}{\beta}\right) C^2_\Omega \|\operatorname{div} y + f\|^2_\Omega. \tag{2.9}$$

Here, y is an arbitrary vector-valued function from $H(\Omega,\mathrm{div})$, β is an arbitrary positive number, and $C_\Omega := c_{1\varepsilon}^{-2}\, C^2_{F\Omega}$, where $c_{1\varepsilon}$ is as in (2.7) and $C_{F\Omega}$ is the Friedrichs constant for the domain Ω, *i.e.*,

$$C_{F\Omega} := \sup_{w \in V_0 \setminus \{0\}} \frac{\|w\|_\Omega}{\|\nabla w\|_\Omega}.$$

Our goal is to deduce an upper bound of the error which also includes the error generated by the simplification of the model.

Theorem 2.1. *The total error is bounded from above by the sum*

$$\|\nabla(u - u_{\varepsilon,h})\|_A \le E^{\varepsilon,\,h}_{\mathrm{disc}} + E^\varepsilon_{\mathrm{mod}}, \tag{2.10}$$

where $E^{\varepsilon,\,h}_{\mathrm{disc}}$ and $E^\varepsilon_{\mathrm{mod}}$ represent the discretization and modeling parts of the error, respectively, and are defined and estimated as follows:

$$E^{\varepsilon,\,h}_{\mathrm{disc}} := \|\nabla(u_\varepsilon - u_{\varepsilon,\,h})\|_A \le \kappa_1\, \mathcal{M}_\Omega(u_{\varepsilon,h},\, y,\, \beta), \tag{2.11}$$

$$E^\varepsilon_{\mathrm{mod}} := \|\nabla(u - u_\varepsilon)\|_A \le \kappa_\varepsilon \left(\frac{\kappa_2}{2}\, \mathcal{M}^2_\Omega(u_{\varepsilon,h},\, y,\, \beta) + \int\limits_\Omega f\, u_{\varepsilon,\,h}\right)^{1/2}, \tag{2.12}$$

where $\kappa_1^2 := 1 + \rho(\Lambda_\varepsilon - I)$, $\kappa_\varepsilon^2 := \frac{2\,\kappa_2}{2\,\kappa_2 - 1}\, \rho(\Lambda_\varepsilon + \Lambda_\varepsilon^{-1} - 2I)$, $\Lambda_\varepsilon := A_\varepsilon^{-1/2} A A_\varepsilon^{-1/2}$, I is the identity matrix, ρ is defined by (2.3)*, and $\kappa_2 := \mu_{\min}$ (see* (2.17)*) if $\mathcal{M}_\Omega$ is positive.*

Proof. By the triangle inequality, we obtain

$$\|\nabla(u - u_{\varepsilon,\,h})\|_A \le \|\nabla(u_\varepsilon - u_{\varepsilon,\,h})\|_A + \|\nabla(u - u_\varepsilon)\|_A = E^{\varepsilon,\,h}_{\mathrm{disc}} + E^\varepsilon_{\mathrm{mod}}. \tag{2.13}$$

We estimate the term $E^{\varepsilon,\,h}_{\mathrm{disc}} = \|\nabla(u_\varepsilon - u_{\varepsilon,\,h})\|_A$ as follows:

$$\begin{aligned}
\left(E^{\varepsilon,\,h}_{\mathrm{disc}}\right)^2 &= \|\nabla(u_\varepsilon - u_{\varepsilon,\,h})\|^2_{A_\varepsilon} + \int\limits_\Omega (A - A_\varepsilon)\, \nabla(u_\varepsilon - u_{\varepsilon,\,h}) \cdot \nabla(u_\varepsilon - u_{\varepsilon,\,h}) \\
&= \|\nabla(u_\varepsilon - u_{\varepsilon,\,h})\|^2_{A_\varepsilon} + \int\limits_\Omega (\Lambda_\varepsilon - I) A_\varepsilon^{1/2} \nabla(u_\varepsilon - u_{\varepsilon,\,h}) \cdot A_\varepsilon^{1/2}\, \nabla(u_\varepsilon - u_{\varepsilon,\,h}) \\
&\le \big(1 + \rho(\Lambda_\varepsilon - I)\big) \|\nabla(u_\varepsilon - u_{\varepsilon,\,h})\|^2_{A_\varepsilon}.
\end{aligned}$$

Since the last norm is estimated by (2.9), we arrive at (2.11). To estimate the term $E^{\varepsilon}_{\mathrm{mod}}$, we note that

$$0 = b\,(u\,-\,u_\varepsilon,\,v)\,+\,(b\,-\,b_\varepsilon)\,(u_\varepsilon,\,v),\qquad \forall\, v \in V_0$$

and choose $v\,=\,u\,-\,u_\varepsilon$. Then,

$$\begin{aligned}(E^{\varepsilon}_{\mathrm{mod}})^2 = \|\nabla(u\,-\,u_\varepsilon)\|^2_A = b\,(u\,-\,u_\varepsilon,\,u\,-\,u_\varepsilon)\,&=\,(b_\varepsilon\,-\,b)(u_\varepsilon,\,u\,-\,u_\varepsilon)\\ &= \int\limits_\Omega (A_\varepsilon\,-\,A)\,\nabla u_\varepsilon\,\cdot\,\nabla(u\,-\,u_\varepsilon).\end{aligned}$$

By the Cauchy-Schwarz inequality, we find that

$$\|\nabla(u\,-\,u_\varepsilon)\|^2_A \le \left(\int\limits_\Omega (A_\varepsilon - A)\,A^{-1}(A_\varepsilon - A)\nabla u_\varepsilon\cdot\nabla u_\varepsilon\right)^{1/2} \|\nabla(u\,-\,u_\varepsilon)\|_A.$$

Hence,

$$\begin{aligned}\|\nabla(u-u_\varepsilon)\|^2_A &\le \int\limits_\Omega (A_\varepsilon - A)A^{-1}(A_\varepsilon - A)\nabla u_\varepsilon\cdot\nabla u_\varepsilon\\ &= \int\limits_\Omega (\Lambda_\varepsilon + \Lambda_\varepsilon^{-1} - 2I)A_\varepsilon^{1/2}\nabla u_\varepsilon\cdot A_\varepsilon^{1/2}\nabla u_\varepsilon \;\le\; \rho\,(\Lambda_\varepsilon + \Lambda_\varepsilon^{-1} - 2I)\,\|\nabla u_\varepsilon\|^2_{A_\varepsilon}.\end{aligned}$$

Further, by the Young inequality with an arbitrary $\mu > 0$, we obtain

$$\begin{aligned}\|\nabla u_\varepsilon\|^2_{A_\varepsilon} &= \int\limits_\Omega f\,(u_\varepsilon - u_{\varepsilon,\,h})\,+\,\int\limits_\Omega f\,u_{\varepsilon,\,h}\;=\;\int\limits_\Omega A_\varepsilon\,\nabla\,u_\varepsilon\cdot\nabla(u_\varepsilon - u_{\varepsilon,\,h})\,+\,\int\limits_\Omega f\,u_{\varepsilon,\,h}\\ &\le \frac{\mu}{2}\,\|\nabla\,u_\varepsilon\|^2_{A_\varepsilon}\,+\,\frac{1}{2\,\mu}\,\|\nabla(u_\varepsilon - u_{\varepsilon,\,h})\|^2_{A_\varepsilon}\,+\,\int\limits_\Omega f\,u_{\varepsilon,\,h}.\end{aligned}$$

For $\mu > \frac{1}{2}$, we have

$$\|\nabla u_\varepsilon\|^2_{A_\varepsilon} \le \frac{\mu^2}{2\,\mu - 1}\,\|\nabla\,(u_\varepsilon - u_{\varepsilon,h})\,\|^2_{A_\varepsilon}\,+\,\frac{2\,\mu}{2\,\mu-1}\int\limits_\Omega f\,u_{\varepsilon,\,h}. \tag{2.14}$$

Therefore,

$$\|\nabla(u\,-\,u_\varepsilon)\|^2_A \le \rho\,(\Lambda_\varepsilon + \Lambda_\varepsilon^{-1} - 2I)\left(\frac{\mu^2}{2\,\mu-1}\,\|\nabla\,(u_\varepsilon - u_{\varepsilon,h})\,\|^2_{A_\varepsilon}\,+\,\frac{2\,\mu}{2\,\mu-1}\int\limits_\Omega f\,u_{\varepsilon,\,h}\right). \tag{2.15}$$

Finally, we estimate the first term of (2.15) by the error majorant and obtain for the modeling error estimate from (2.9)

$$\left(E^{\varepsilon}_{\mathrm{mod}}\right)^2 = \|\nabla(u\,-\,u_\varepsilon)\|_A \le \frac{2\,\mu}{2\,\mu-1}\,\rho(\Lambda_\varepsilon + \Lambda_\varepsilon^{-1} - 2I)\left(\frac{\mu}{2}\,\mathcal{M}^2_\Omega(u_{\varepsilon,h},\,y,\,\beta) + \int\limits_\Omega f\,u_{\varepsilon,\,h}\right). \tag{2.16}$$

Hence, $E^{\varepsilon}_{\mathrm{mod}}$ can be minimized with respect to $\mu > 1/2$. Easy calculations show that $E^{\varepsilon}_{\mathrm{mod}}$ has the unique local minimum

$$\mu = \mu_{\min} = \frac{1}{2}\,+\,\left(\frac{1}{4}\,+\,\frac{\int\limits_\Omega f\,u_{\varepsilon,\,h}}{\mathcal{M}^2_\Omega(u_{\varepsilon,h},\,y,\,\beta)}\right)^{1/2}, \tag{2.17}$$

provided that $\mathcal{M}^2_\Omega(u_{\varepsilon,h},\, y,\, \beta)$ is positive, otherwise

$$\left(E^\varepsilon_{\rm mod}\right)^2 \le \rho(\Lambda_\varepsilon + \Lambda_\varepsilon^{-1} - 2I) \int\limits_\Omega f\, u_{\varepsilon,\,h},$$

which is also encompassed in (2.17) if we formally set $\mu_{\min} = +\infty$. Now we obtain (2.12) by (2.16) and (2.17). The estimate (2.10) follows from (2.13). □

Remark 2.2. Alternatively, we could have estimated the error $\|\nabla(u - u_{\varepsilon,h})\|_A$ directly by the error majorant. However, the first term then contains the inverse A^{-1} of the original matrix (instead of A_ε^{-1}). This fact leads to two essential drawbacks. First, computations related to the majorant with A would require complicated integration procedures (especially if the problem contains fine structures). For this reason, it is much simpler to find a suitable y and to evaluate the majorant of A_ε instead of A. Another point is that the estimate (2.10) includes two meaningful quantities (discretization and modeling errors). They are explicitly estimated by (2.11) and (2.12) what allows us to balance these errors with the help of an adaptive method described in Section 2.2.

Remark 2.3. From (2.10), it follows that

$$\|\nabla(u\, -\, u_{\varepsilon,h})\|_A \le \left(\kappa_1 + \frac{\sqrt{\kappa_2}}{\sqrt{2}}\,\kappa_\varepsilon\right) \mathcal{M}_\Omega(u_{\varepsilon,h},\, y,\, \beta) + \kappa_\varepsilon \left(\int\limits_\Omega f\, u_{\varepsilon,\,h}\right)^{1/2}. \tag{2.18}$$

We note that the coefficient κ_ε can be viewed as a measure of how accurately A_ε approximates A. In order to obtain a converging algorithm the sequence of simplified interfaces and the corresponding averaging strategy (used in the definition of A_ε) should be selected such that $\kappa_\varepsilon \to 0$ as $\varepsilon \to 0$. Since κ_ε is defined as a supremum over local quantities its behavior gives an information about the parts of Ω, where A_ε should be improved. It is easy to see that if $A = A_\varepsilon$, then $\Lambda_\varepsilon = \Lambda_\varepsilon^{-1} = I$, and $\kappa_1 = 1$, $\kappa_\varepsilon = 0$. In this case, the term related to the modeling error vanishes and the right-hand side of (2.10) is completely determined by the discretization error.

If A and A_ε are diagonal matrices, then $\Lambda_\varepsilon = \{\lambda^\varepsilon_{ij}\}$ is also diagonal and $\lambda^\varepsilon_{ii} = \frac{a_{ii}}{a^\varepsilon_{ii}}$. In this case, we can easily find the quantities

$$\kappa_1^2 = 1 + \rho\,(\Lambda_\varepsilon - I) = 1 + \sup_{x\in\Omega} \max_{i=1,\dots,d} \frac{|a_{ii}\,(x) - a^\varepsilon_{ii}\,(x)\,|}{a^\varepsilon_{ii}\,(x)}, \tag{2.19}$$

$$\kappa_\varepsilon^2 = \kappa_2\,\rho\left(\Lambda_\varepsilon + \Lambda_\varepsilon^{-1} - 2I\right) = \kappa_2 \sup_{x\in\Omega} \max_{i=1,\dots,d} \frac{(a_{ii}\,(x) - a^\varepsilon_{ii}\,(x))^2}{a_{ii}\,(x)\,a^\varepsilon_{ii}\,(x)}. \tag{2.20}$$

3. Modeling-discretization adaptivity and *a posteriori* error estimation

3.1. Sequence of simplified models

Henceforth, we assume that the diffusion coefficients are piecewise constant, Ω is decomposed into connected non overlapping subsets ω_i, $0 \le i \le q$ (called "inclusions"). By $\mathcal{H}$ and γ we denote the sets of all inclusions and their interfaces, respectively, *i.e.*,

$$\mathcal{H} := \{\omega_i :\, 0 \le i \le q\} \quad \text{and} \quad \gamma := \bigcup_{\omega\in\mathcal{H}} \partial\omega.$$

For a hierarchical modeling we introduce a sequence of resolutions for the interfaces along the discontinuities of the diffusion matrix.

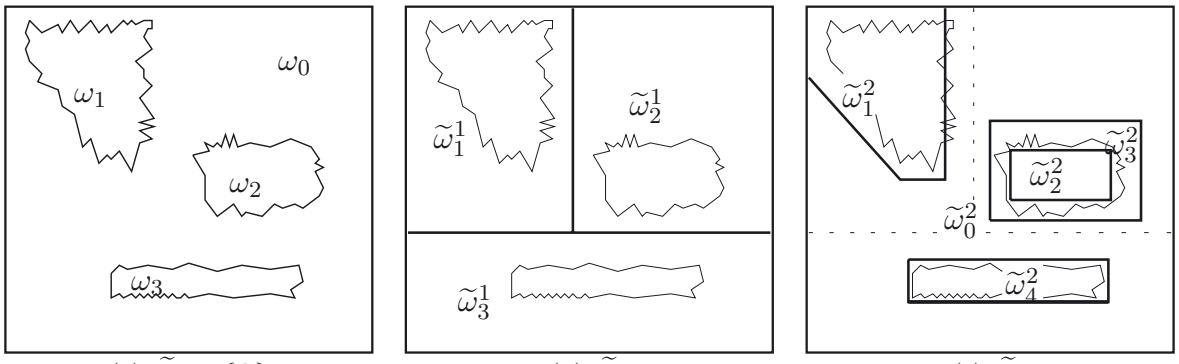

(a) $\widetilde{\mathcal{H}}_0 = \{\Omega\}$ (b) $\widetilde{\mathcal{H}}_1$ (c) $\widetilde{\mathcal{H}}_2$

FIGURE 2. Example of the first three refinements.

Assumption 3.1. *A sequence of resolutions $\widetilde{\mathcal{H}_j}$, $j = 0, 1, \ldots, J$, for the inclusions from $\mathcal{H}$ (illustrated in Fig. 2) satisfy the following conditions:*

1. $\widetilde{\mathcal{H}}_0 = \{\Omega\}$;
2. $\widetilde{\mathcal{H}}_j = \left\{\widetilde{\omega}_k^j : \ 0 \le k \le \tilde{q}_j\right\}$ *is a disjoint partitioning of Ω, i.e.,*
   (a) *all $\widetilde{\omega}^j \in \widetilde{\mathcal{H}_j}$ are open subsets of Ω,*
   (b) $\overline{\Omega} = \overline{\bigcup_{\widetilde{\omega} \in \widetilde{\mathcal{H}}_j} \widetilde{\omega}}$;
3. *The final level $\widetilde{\mathcal{H}}_J$ equals $\mathcal{H}$ or is a refinement of $\mathcal{H}$, i.e.,*

$$\forall\, \widetilde{\omega}^J \in \widetilde{\mathcal{H}}_J \quad \exists \omega \in \mathcal{H} : \ \widetilde{\omega}^J \subset \omega \ .$$

Further we define simplified, $\widetilde{\mathcal{H}}_l$-piecewise constant coefficients A_ε as suitable averages of A. For $\widetilde{\omega}^l \in \widetilde{\mathcal{H}}_l$ the subset

$$\widetilde{\mathcal{H}}_{\widetilde{\omega}^l} := \{\omega \in \mathcal{H} : \ |\omega \cap \widetilde{\omega}^l| > 0\}$$

contains those (exact) inclusions which are influencing A_ε locally on $\widetilde{\omega}^l$. Furthermore, we denote by $\overline{\omega}_l \in \widetilde{\mathcal{H}}_{\widetilde{\omega}^l}$ some fixed inclusion which satisfies

$$\text{area}\,(\overline{\omega}_l) = \max\left\{\text{area}\,(\omega_l) : \omega_l \in \widetilde{\mathcal{H}}_{\widetilde{\omega}^l}\right\}.$$

We also denote by $\#\widetilde{\mathcal{H}}_{\widetilde{\omega}^l}$ the cardinality of $\widetilde{\mathcal{H}}_{\widetilde{\omega}^l}$. Some popular "averaging" strategies are then given by:

(1) $A_\varepsilon|_{\widetilde{\omega}^l} := A|_{\overline{\omega}_l}$, (value of the coefficient in the inclusion with the maximal area in the influence region);

(2) $A_\varepsilon|_{\widetilde{\omega}^l} := \frac{1}{\#\widetilde{\mathcal{H}}_{\widetilde{\omega}^l}} \sum_{i=0}^{\#\widetilde{\mathcal{H}}_{\widetilde{\omega}^l}} A|_{\omega_i}$, (arithmetic mean);

(3) $A_\varepsilon|_{\widetilde{\omega}^l} := \left(\frac{1}{\#\widetilde{\mathcal{H}}_{\widetilde{\omega}^l}} \sum_{i=0}^{\#\widetilde{\mathcal{H}}_{\widetilde{\omega}^l}} (A|_{\omega_i})^{-1}\right)^{-1}$, (harmonic mean);

(4) $A_\varepsilon|_{\widetilde{\omega}^l} := \frac{1}{|\widetilde{\omega}^l|} \int_{\widetilde{\omega}^l} A$, (arithmetic integral mean);

(5) $A_\varepsilon|_{\widetilde{\omega}^l} := \left(\frac{1}{|\widetilde{\omega}^l|} \int_{\widetilde{\omega}^l} A^{-1}\right)^{-1}$, (harmonic integral mean).

Remark 3.2. As one could predict the strategy (1) (based on using the values of the inclusions with the maximal area in the corresponding influence regions) is rather coarse and averaging (harmonic and arithmetic) leads to better results (see Test 1.4 in Sect. 4.1).

Remark 3.3. Problems with fine periodical structures form a special class of problems with complicated coefficients, which are usually considered within the framework of the homogenization theory. From the literature (*cf.* [13], Chap. 8) it is known that for fine periodic structures in the one dimensional case, the best averaging strategy is the harmonic integral mean. In the two dimensional case, proper averaging depends on the structure of the matrix and solution of a boundary value problem on the cell (see [8, 14, 16]). In principle the numerical strategy considered in this paper can be applied to periodic structures including the case, where the number of cells is not large enough for the homogenized model to give a satisfactory accuracy. If the periodical structure is fine then it is reasonable to use the corresponding homogenized problem but this is not the case we are focused on.

3.2. Computation of the majorant

To estimate the errors $E^{\varepsilon,h}_{\rm disc}$ and $E^{\varepsilon}_{\rm mod}$, we need to evaluate the term $\mathcal{M}^2_{\Omega}(u_{\varepsilon,h}, y, \beta)$ (*cf.* Thm. 2.1) for a proper flux approximation y and a parameter β. The questions, how to choose β and how to compute the flux approximation y from the discrete solution $u_{\varepsilon_l,h}$, have been considered in the literature (see, *e.g.*, [18, 19, 22, 25–27, 34]). Below we briefly discuss the application to our case. In accordance with (2.10) any choice of $(\beta, y) \subset \mathbb{R} \times H(\Omega, \mathrm{div})$ in the error majorant results in an upper bound of the error. However, sharp estimates require a proper choice of these quantities, which has to balance the extra computational cost with the benefit of sharper estimates.

If A, A_ε, f, and C_Ω are known, then the squared majorant $\mathcal{M}^2_{\Omega}(u_{\varepsilon,h}, y, \beta)$ is a quadratic functional. Our goal is to find some $y_h \in S^2_h$ and $\beta \in \mathbb{R}$ such that $\mathcal{M}^2_{\Omega}(u_{\varepsilon,h}, y_h, \beta)$ is close to the minimum over $y \in H(\Omega, \mathrm{div})$ and $\beta \in \mathbb{R}$. For the corresponding iterative algorithm, we introduce the following notation:

For every vertex ξ of $\mathcal{T}_h$, denote by $\mathcal{P}_\xi := \{\tau \in \mathcal{T}_h : \xi \in \overline{\tau}\}$ the neighboring elements, by $\omega_\xi := \overline{\bigcup\limits_{\tau\in\mathcal{P}_\xi} \tau}$ the patch of this vertex and define $y^{(0)}_h \in S^2_h$ by the patchwise flux averaging using the nodal condition

$$y^{(0)}_h(\xi) := \frac{1}{|\omega_\xi|} \int_{\omega_\xi} A_\varepsilon \nabla u_{\varepsilon,h}. \tag{3.1}$$

Let b_j denote the usual hat function for the vertices ξ_j, $1 \le j \le N$, of $\mathcal{T}_h$, and $S_j := \mathrm{span}\{(b_j, 0), (0, b_j)\} \subset S^2_h$.

Algorithm 1 (global minimization of the error majorant)**.**

Set $y^{(0)}_h(\xi) = \frac{1}{|\omega_\xi|} \int_{\omega_\xi} A_\varepsilon \nabla u_{\varepsilon,h}$ and $\beta^{(0)} = \frac{C_\Omega \|\mathrm{div}\, y^{(0)}_h + f_h\|_\Omega}{\|A_\varepsilon \nabla u_{\varepsilon,h} - y^{(0)}_h\|_{A^{-1}_\varepsilon}}$.

Choose $\nu_{\max}$.

For $\nu = 1$ to $\nu_{\max}$ do begin

$$y^{(\nu)}_h = \operatorname*{argmin}_{v\in S^2_h} \mathcal{M}^2_{\Omega}(u_{\varepsilon,h}, v, \beta^{(\nu-1)}). \tag{3.2}$$

$$\beta^{(\nu)} = \frac{C_\Omega \|\mathrm{div}\, y^{(\nu)}_h + f_h\|_\Omega}{\|A_\varepsilon \nabla u_{\varepsilon,h} - y^{(\nu)}_h\|_{A^{-1}_\varepsilon}}.$$

end

Calculate $\mathcal{M}^2_{\Omega}(u_{\varepsilon,h}, y^{(\nu_{\max})}_h, \beta^{(\nu_{\max})})$.

The numerical experiments in Section 4 shows that the choice $\nu_{\max} = 1$ is sufficient for all considered cases.

Algorithm 2 (local minimization of the error majorant)**.**

Set $y_h^{(0)}(\xi) = \frac{1}{|\omega_\xi|}\int_{\omega_\xi} A_\varepsilon \nabla u_{\varepsilon,h}$ and $\beta^{(0)} = \frac{C_\Omega \|\operatorname{div} y_h^{(0)} + f_h\|_\Omega}{\|A_\varepsilon \nabla u_{\varepsilon,h} - y_h^{(0)}\|_{A_\varepsilon^{-1}}}$.

Choose $\nu_{\max}$ and $\iota_{\max}$.

For $\nu = 1$ to $\nu_{\max}$ do begin

Set $\gamma_N^{(0)} = y_h^{(\nu-1)}$.

For $i = 1$ to $\iota_{\max}$ do begin

$$\begin{aligned}
&\gamma_0^{(i)} = \gamma_N^{(i-1)}.\\
&\text{For } j = 1 \text{ to } N \text{ do begin}\\
&\quad v_j = \operatorname*{argmin}_{v \in S_j^2} \mathcal{M}_\Omega^2(u_{\varepsilon,h},\, \gamma_{j-1}^{(i)} + v, \beta^{(\nu-1)}).\\
&\quad \gamma_j^{(i)} = \gamma_{j-1}^{(i)} + v_j.\\
&\text{end}
\end{aligned} \tag{3.3}$$

Set $y_h^{(\nu)} = \gamma_N^{(\iota_{\max})}$ and $\beta^{(\nu)} = \frac{C_\Omega \|\operatorname{div} y_h^{(\nu)} + f_h\|_\Omega}{\|A_\varepsilon \nabla u_{\varepsilon,h} - y_h^{(\nu)}\|_{A_\varepsilon^{-1}}}$.

end

Calculate $\mathcal{M}_\Omega^2(u_{\varepsilon,h},\, y_h^{(\nu_{\max})}, \beta^{(\nu_{\max})})$.

The numerical experiments in Section 4 shows that the choices $\nu_{\max} = 1$ and $\iota_{\max} = 3$ are sufficient for all considered cases. Note that the global minimization requires the generation and solution of a linear system of dimension $2N$. On the one hand, we expect that the arising computational cost is of the same order as the cost for computing $u_{\varepsilon,h}$. On the other hand, the memory requirements are reduced in Algorithm 2 on the expense of less sharp estimates.

4. Numerical results

In this section, we demonstrate the performance of the combined modeling-discretization adaptive strategy for the case of a linear diffusion problem with a discontinuous, non-homogeneous, piecewise constant diffusion coefficient, which has rather complex interfaces separating its discontinuities and is represented by a symmetric, non-diagonal matrix.

In the following experiments, we consider the domain $\Omega = (0,\, 1)^2$ with an inclusion ω_1 (*cf.* Fig. 3). We choose

$$A|_{\omega_1} = 2\,I \quad \text{and} \quad A|_{\omega_0} = I \tag{4.1}$$

and note that the exact structure of A can be resolved on the uniform mesh with $h = 2^{-8}$.

The right-hand side of the diffusion equation is given by

$$f(x,\, y) = 2x\,(1 - x) + 2y\,(1 - y). \tag{4.2}$$

Remark 4.1. If one solves this diffusion problem with standard $\mathbb{P}_1$ finite elements on a coarse mesh which does not resolve the discontinuities in A, then the quadrature for setting up the stiffness matrix either becomes very expensive (depending on the "roughness" of the interface) or prohibitive inaccurate. The numerical example has mainly the purpose to illustrate the behavior and sharpness of our modeling-discretization error estimator as well as the proper selection of the control parameters.

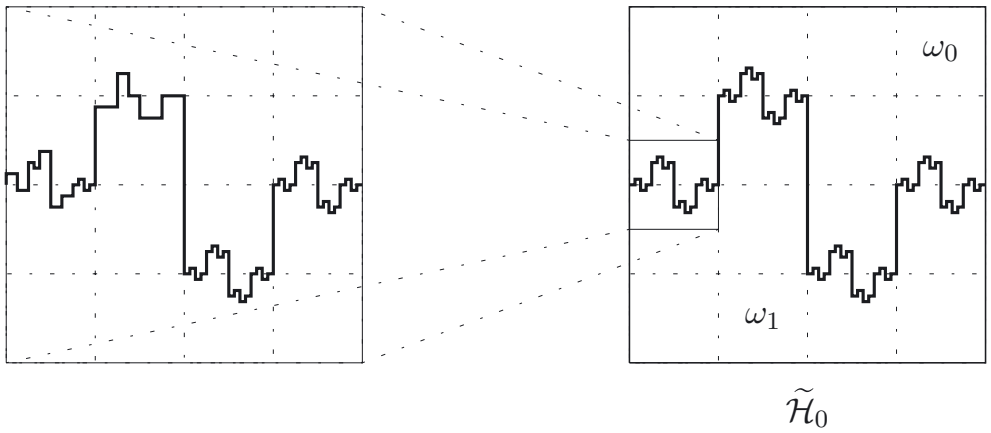

FIGURE 3. Exact geometry of domain Ω.

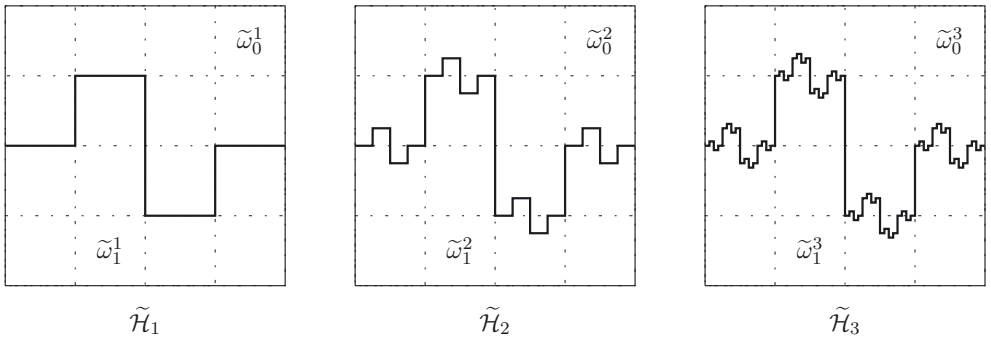

FIGURE 4. Hierarchy of geometries of simplified models.

We construct a series of Models 1–3, in which Model 1 is the coarsest model and Model 4 is the finest one. The corresponding diffusion matrices are denoted by A_{ε_1}, A_{ε_2}, and A_{ε_3}, respectively. They are defined on the corresponding resolution levels $\widetilde{\mathcal{H}}_1$ to $\widetilde{\mathcal{H}}_3$ (*cf.* Fig. 4) by using the first simplification strategy from Section 3.1, *i.e.*,

$$A_{\varepsilon_i}|_{\widetilde{\omega}_j^i} := A|_{\overline{\omega}_j^i}, \qquad \widetilde{\omega}_j^i \in \widetilde{\mathcal{H}}_i, \quad \overline{\omega}_j^i \in \widetilde{\mathcal{H}}_{\widetilde{\omega}_j^i}, \quad i = 1, 2, 3,\ j = 0, 1. \tag{4.3}$$

The exact structure of the first (coarsest) model A_{ε_1} can be resolved on the mesh with $h = 2^{-2}$, in the case of A_{ε_2} it is necessary to set $h = 2^{-4}$ and in the case of A_{ε_3} we must have $h = 2^{-6}$. Then the exact problem (2.1) is replaced by its simplified counterparts associated with different resolution levels.

All numerical tests presented below were made on a SUN processor RX900 with 8 × Intel Xeon X7550 (8 Cores, 16 Threads) CPU, 2.0 GHz (Turbo: 2.4 GHz) and 512 GB main memory.

4.1. Test series 1

Below we present results of computer simulation that demonstrate the efficiency of the minimization strategies (3.1)–(3.3) for this problem.

Test 1.1. We select Model 1, set $h = 2^{-5}$, use a GMRES-Solver to find an approximate solution, and estimate the total error by the combined modeling-discretization error majorant $\mathscr{M}$ (*cf.* Sect. 3.2) defined here by

$$\mathscr{M} := E_{\mathrm{disc}}^{\varepsilon,h} + \left(\left(E_{\mathrm{mod}^1}^{\varepsilon}\right)^2 + \left(E_{\mathrm{mod}^2}^{\varepsilon}\right)^2 \right)^{1/2}, \tag{4.4}$$

where

$$E^{\varepsilon}_{\mathrm{mod}^1} := \Big(\frac{\kappa_2}{2}\Big)^{1/2} \kappa_\varepsilon \, \mathcal{M}_\Omega(u_{\varepsilon,h},\, y,\, \beta) \quad \text{and} \quad E^{\varepsilon}_{\mathrm{mod}^2} := \kappa_\varepsilon \left(\int_\Omega f\, u_{\varepsilon,h} \right)^{1/2}$$

(*cf.* (2.12)). The first term has been computed by the approximative (local) and global minimization strategies (see Sect. 3.2).

The parameters of the local minimization algorithm are $\iota_{\max}$ and $\nu_{\max}$. In our first test, we set $\nu_{\max} = 1$ and vary $\iota_{\max}$ from 0 to 9. The first line of Table 1 corresponds to the case in which y is constructed by simple flux averaging (3.1). Table 1 shows that $\iota_{\max} = 3$ is enough for getting accurate values of $\mathscr{M}$ and further iterations ($\iota_{\max} = 6$ to $\iota_{\max} = 9$) do not significantly improve it. Analogous tests with the other models have shown similar results.

TABLE 1. The majorant $\mathcal{M}$ with the corresponding parts and CPU required for optimization of the flux function (Model 1 for $\nu_{\max} = 1$).

$\iota_{\max}$	β_1	$E^{\varepsilon,h}_{\mathrm{disc}}$	$E^{\varepsilon}_{\mathrm{mod}^1}$	$E^{\varepsilon}_{\mathrm{mod}^2}$	$\mathscr{M}$	t, (s)
0	1.92	0.0381	0.0073	0.0502	0.0987	1.6
3	0.57	0.0194	0.0062	0.0185	0.0389	6.85
6	0.52	0.0184	0.0062	0.0185	0.0379	15.41
9	0.50	0.0183	0.0062	0.0185	0.0378	20.75

TABLE 2. The error majorant and CPU time in seconds required for optimization of the flux function in the case of Model 1 for $\iota_{\max} = 3$.

$\nu_{\max}$	$\beta_{\nu_{\max}}$	$E^{\varepsilon,h}_{\mathrm{disc}}$	$E^{\varepsilon}_{\mathrm{mod}^1}$	$E^{\varepsilon}_{\mathrm{mod}^2}$	$\mathscr{M}$	t, (s)
1	0.57	0.0194	0.0062	0.0185	0.0389	6.85
2	0.51	0.0184	0.0062	0.0185	0.0379	14.45
3	0.48	0.0182	0.0062	0.0185	0.0377	22.57

Test 1.2. In this series of numerical experiments, we set $\iota_{\max} = 3$ and increase the parameter $\nu_{\max}$. The corresponding results are presented in Table 2. They demonstrate that increasing of $\nu_{\max}$ does not significantly improve the majorant. For this reason by using the approximative (local) minimization strategy from Algorithm 2, it is sufficient to choose $\iota_{\max} = 3$ and $\nu_{\max} = 1$.

Test 1.3. In this test, we analyze efficiency of the global minimization strategy. We solve the four selected approximate models on the meshes with $h = 2^{-4}$, 2^{-5}, 2^{-6}, 2^{-7} and evaluate the error majorant by using of the local (with $\iota_{\max} = 3$ and $\nu_{\max} = 1$) and global (with $\nu_{\max} = 1$) minimization strategy. The corresponding majorants are denoted by $\mathscr{M}^{\mathrm{loc}}$ and $\mathscr{M}^{\mathrm{glob}}$ respectively. Table 3 presents the results.
As expected the global strategy provides the exacter majorants and should be preferred if the computer allows the treatment of large systems of equations. That is why for our subsequent tests, we choose the global minimization strategy and solve the linear systems with a PARDISO-solver from `http://www.pardiso-project.org/download/academic.cgi`.

Test 1.4. In order to test the sensitivity of the modeling error majorant

$$E^{\varepsilon}_{\mathrm{mod}} = \Big(\big(E^{\varepsilon}_{\mathrm{mod}^1}\big)^2 + \big(E^{\varepsilon}_{\mathrm{mod}^2}\big)^2 \Big)^{1/2}$$

for our simplified models, we investigate how it depends on the strategy used to define a simplified matrix A_ε. In the three experiment below, we use the simplification strategies (1), (4) and (5) presented in Section 3.1.

TABLE 3. Comparison of the error majorant calculated by using different minimization strategies.

$-\log_2 h$	Model 1		Model 2		Model 3	
	$\mathscr{M}^{\mathrm{loc}}$	$\mathscr{M}^{\mathrm{glob}}$	$\mathscr{M}^{\mathrm{loc}}$	$\mathscr{M}^{\mathrm{glob}}$	$\mathscr{M}^{\mathrm{loc}}$	$\mathscr{M}^{\mathrm{glob}}$
4	0.0538	0.0421	0.0569	0.0400	–	–
5	0.0389	0.0316	0.0359	0.0296	–	–
6	0.0333	0.0281	0.0299	0.0266	0.0260	0.0247
7	0.0290	0.0260	0.0278	0.0250	0.0255	0.0240

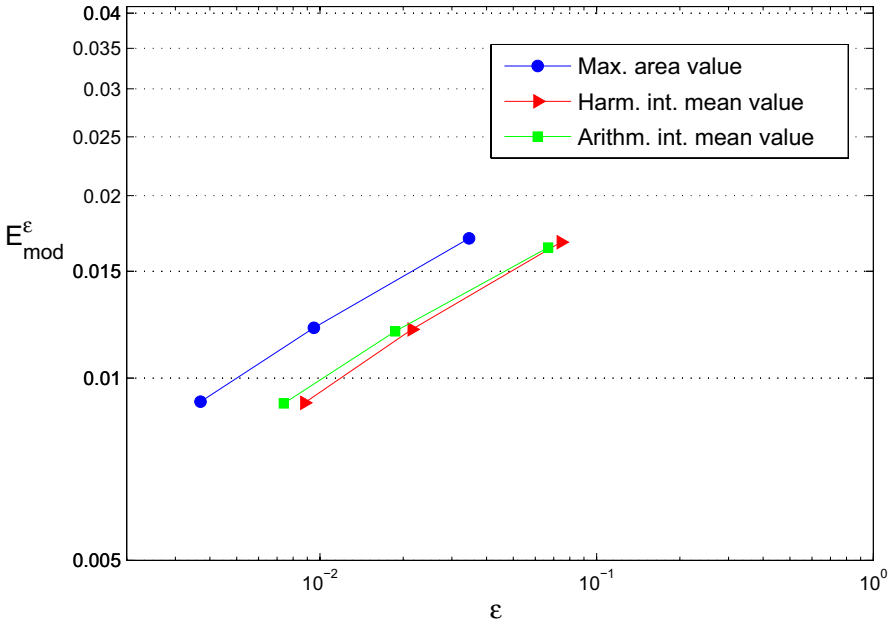

FIGURE 5. Values of modeling errors for different simplification strategies.

From Figure 5 we conclude that $E^{\varepsilon}_{\mathrm{mod}} = \mathcal{O}(k\,\varepsilon^{\nu})$, where $\varepsilon := \|A - A_{\varepsilon}\|_{L^1}$, $\nu \in \mathbb{R}$ is constant for the chosen model hierarchy, and $k \in \mathbb{R}$ only slightly depends on the type of simplification strategy. We see that in this example different simplification strategies generate models with close values of modeling errors. Certainly in other examples, *e.g.* with thin quasi-periodical structure, some particular way of simplification may be preferable.

4.2. Test series 2

Now we present several tests that demonstrate the performance of the adaptive combined modeling-discretization strategy.

Test 2.1. We assume now that the problem (2.1), (4.1)–(4.2) must be solved with a given tolerance δ. Table 3 and Figure 6 show that, *e.g.*, for $\delta = 0.04$ we do not need to solve the exact problem (2.1): indeed Model 2 provides such an accuracy if we set $h = 2^{-4}$. If $\delta = 0.025$ then Model 2 needs $h = 2^{-7}$ but Model 3 only $h = 2^{-6}$ so that using this model is preferable.

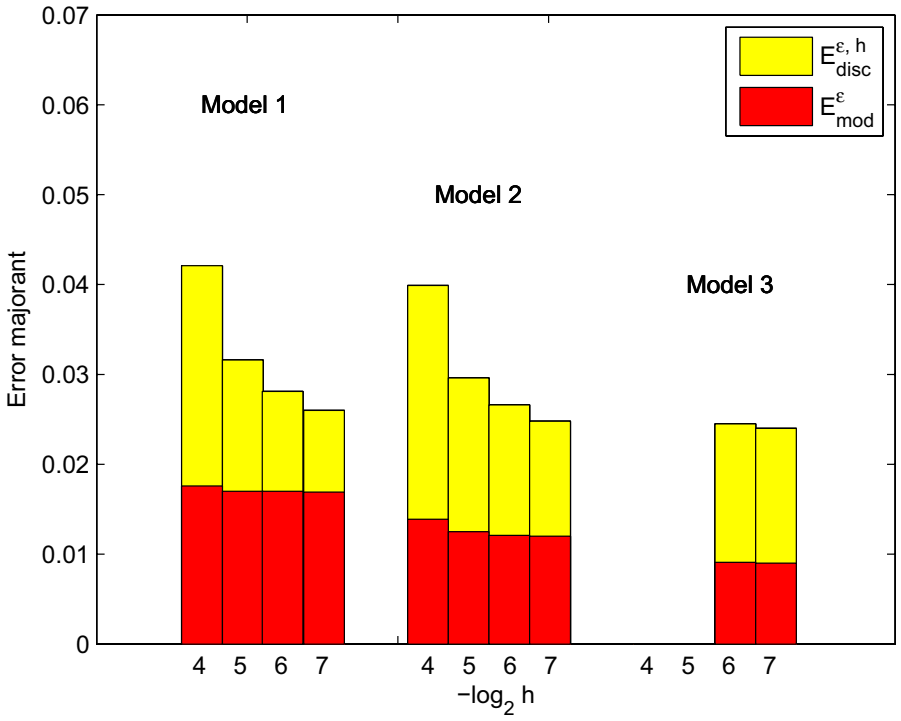

FIGURE 6. Modeling and discretization error majorants for the approximate models.

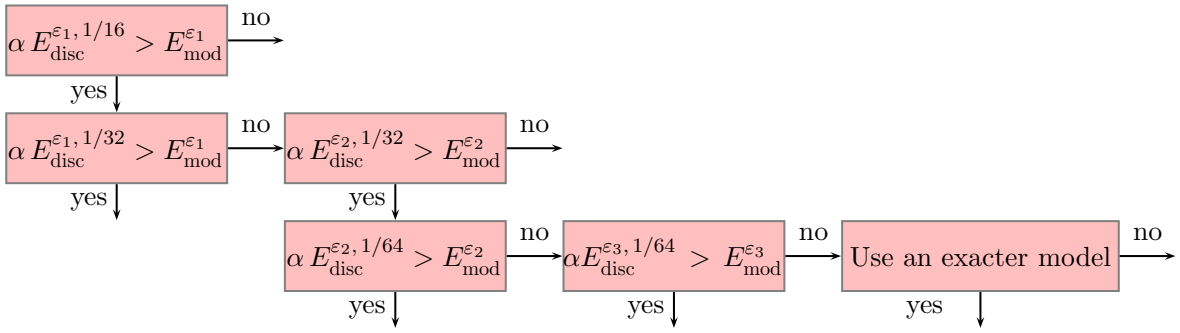

FIGURE 7. Combined modeling-discretization error minimization strategy.

One can find the shortest way to choose the optimal model in the previous test, by using the combined modeling-discretization error minimization strategy from Section 2.2 presented in Figure 7:

Let $\delta = 0.025$. We choose, *e.g.*, $\alpha = 0.8$ and start with Model 1 and $h = 2^{-4}$. In this case we find that $\mathcal{M} > \delta$, $E^{\varepsilon_1}_{\rm mod} < \alpha\, E^{\varepsilon_1,\,1/16}_{\rm disc}$ (*cf.* Fig. 6) and, therefore, should refine the mesh. For the mesh with $h = 2^{-5}$, we obtain $E^{\varepsilon_1}_{\rm mod} > \alpha\, E^{\varepsilon_1,\,1/32}_{\rm disc}$. Hence, we should pass to a more accurate Model 2. For Model 2 with $h = 2^{-5}$, we have $E^{\varepsilon_2}_{\rm mod} < \alpha\, E^{\varepsilon_2,\,1/32}_{\rm disc}$ and, therefore, refine the mesh again. We continue this process unless the required accuracy is achieved.

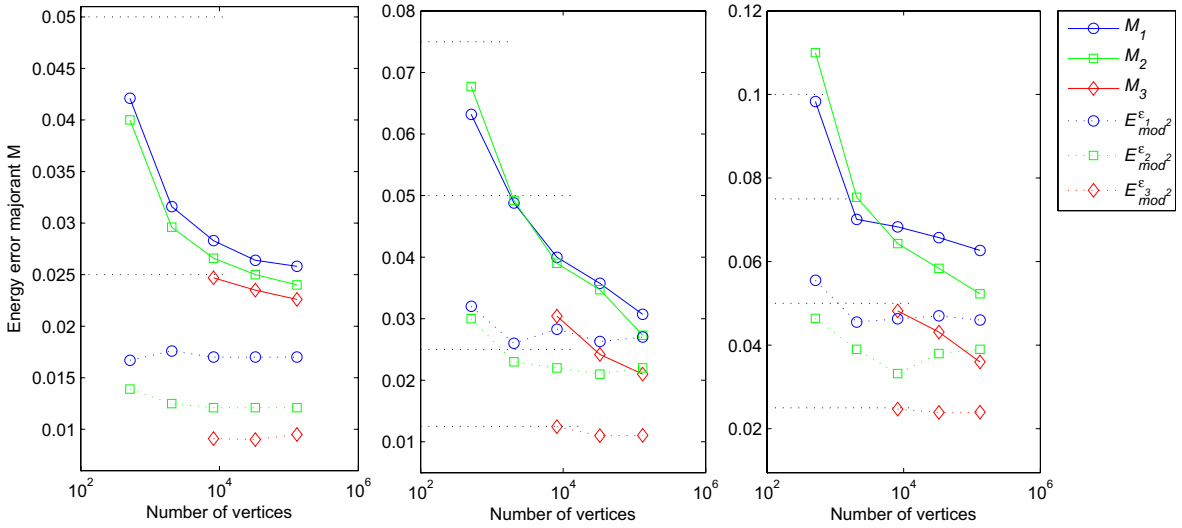

FIGURE 8. Combined modeling-discretization error majorants for $A|_{\omega_0} = I$, $A|_{\omega_1} = 2\,I$ (left), $A|_{\omega_1} = 4\,I$ (middle) and $A|_{\omega_1} = 10\,I$ (right).

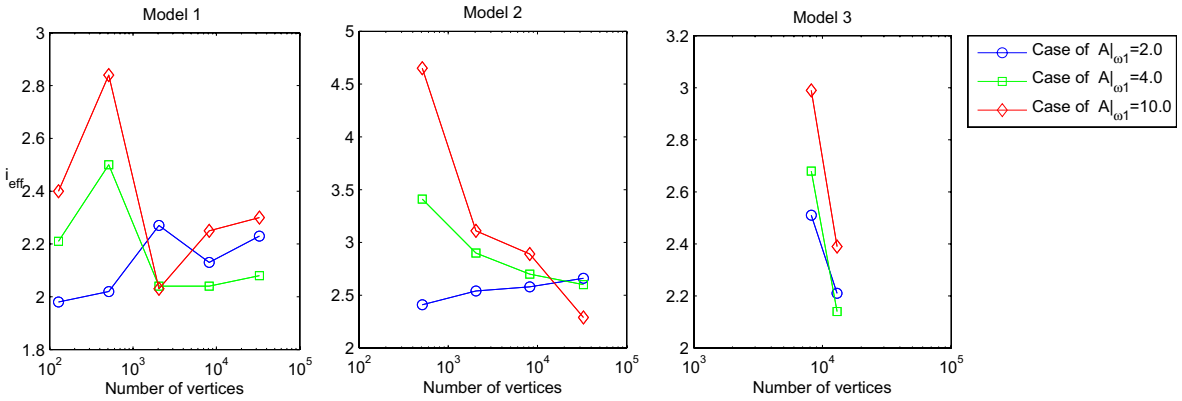

FIGURE 9. Efficiency index for different models.

TABLE 4. Efficiency index of the total error majorants depending on number of vertices.

N	Model 1, $A\|_{\omega_1}$			Model 2, $A\|_{\omega_1}$			Model 3, $A\|_{\omega_1}$		
	$2I$	$4I$	$10I$	$2I$	$4I$	$10I$	$2I$	$4I$	$10I$
128	1.98	2.21	2.40	–	–	–	–	–	–
512	2.02	2.50	2.84	2.41	3.41	4.65	–	–	–
2048	2.27	2.04	2.03	2.54	2.90	3.11	–	–	–
8192	2.13	2.04	2.25	2.58	2.70	2.89	2.51	2.68	2.99
32 768	2.23	2.08	2.30	2.66	2.60	2.29	2.21	2.14	2.39

Test 2.2. We solve each of these three models for the following three cases of the diffusion coefficients:

1. $A|_{\omega_0} = I$ and $A|_{\omega_1} = 2\,I$;
2. $A|_{\omega_0} = I$ and $A|_{\omega_1} = 4\,I$;
3. $A|_{\omega_0} = I$ and $A|_{\omega_1} = 10\,I$,

and estimate the difference between the exact solution of (2.1) and numerical solutions of simplified problems associated with different resolution levels (computed in accordance with Thm. 2.1). The results of these numerical experiments are presented in Figure 8 below. Here, the solid lines correspond to the values of total (modeling plus discretization) errors and the values of modeling errors are depicted below.

We see that an economical numerical strategy indeed requires switching from one model to another one. For example, we see that in the case of

$$A|_{\omega_0} = I,\ A|_{\omega_1} = 4\,I \quad \text{and} \quad A|_{\omega_0} = I,\ A|_{\omega_1} = 10\,I.$$

Model 1 is more advantageous than Model 2 if one solves the diffusion problem using less then 8000 vertices.

Furthermore, if one has to achieve the target accuracy, *e.g.*, $\delta = 0.04$ in the case of

$$A|_{\omega_0} = I,\ A|_{\omega_1} = 10\,I,$$

there is no sense to use Model 1 at all because the modeling error of Model 1 is already larger then the target accuracy.

Test 2.3. To quantify the efficiency of the calculation of the majorant, we must compare $\mathscr{M}$ from (4.4) with the exact error $e := \|\nabla(u - u_{\varepsilon,h})\|_A$. Since the exact solutions are unknown, we follow the commonly accepted way and compute the so-called "reference" solutions $u_{\rm ref}$ on a mesh much finer than any of those used in the error estimation tests. It turns out that for all approximate models the efficiency indices are mainly in the interval [1.9, 2.5] (see Fig. 9 and Tab. 4).

4.3. Conclusions

We have presented a modeling-discretization strategy for elliptic boundary value problems with complicated structure of coefficients in the main part of the differential operator, which is based on explicit evaluation of discretization and modeling errors. Numerical tests exposed (and also many other tests that we have performed) show that approximate solutions with a desirable (engineering) accuracy can often be obtained by using rather coarse models (avoiding difficulties that arise if the exact (most detailed) resolution of the coefficients is used). Finally, we note that similar arguments can be used to evaluate errors caused by incomplete knowledge of coefficients (that may arise due to uncertainties in the problem data) or errors of numerical integration.

References

[1] M. Ainsworth, *A posteriori* error estimation for fully discrete hierarchic models of elliptic boundary value problems on thin domains. *Numer. Math.* **80** (1998) 325–362.

[2] M. Ainsworth and A. Arnold, A reliable *a posteriori* error estimator for adaptive hierarchic modeling, in *Adv. Adap. Comp. Meth. Mech.*, edited by P. Ladevéze and J.T. Oden (1998) 101–114.

[3] M. Ainsworth and J.T. Oden, *A Posteriori Error Estimation in Finite Element Analysis*. Wiley (2000).

[4] I. Babuška and W.C. Rheinboldt, *A posteriori* error estimates for the finite element method. *Int. J. Numer. Math. Eng.* **12** (1978) 1597–1615.

[5] I. Babuška and W.C. Rheinboldt, Error estimates for adaptive finite element computations. *SIAM J. Numer. Anal.* **15** (1978) 736–754.

[6] I. Babuška and R. Rodríguez, The problem of the selection of an *a posteriori* error indicator based on smoothing techniques. *Int. J. Numer. Methods Eng.* **36** (1993) 539–567.

[7] I. Babuška and C. Schwab, *A posteriori* error estimation for hierarchic models of elliptic boundary value problems on thin domains. *SIAM J. Numer. Anal.* **33** (1996) 221–246.

[8] A. Bensoussan, J.-L. Lions and G. Papanicolaou, *Asymptotic Analysis for Periodic Structures*. Amsterdam, North-Holland (1978).

[9] D. Braess, *Finite elements: Theory, Fast Solvers and Application in Solid Mechanics*. Cambridge University Press (2007).

[10] D. Braess, An *a posteriori* error estimate and a comparison theorem for the nonconforming P1 element. *Calcolo* **46** (2009) 149–155.

[11] D. Braess and J. Schöberl, Equilibrated residual error estimator for edge elements. *Math. Comp.* **77** (2008) 651–672.

[12] C. Carstensen and S. Sauter, *A posteriori* error analysis for elliptic PDEs on domains with complicated structures. *Numer. Math.* **96** (2004) 691–721.

[13] M. Chipot, *Elliptic Equations: An Introductory Course*. Birkhäuser Verlag AG (2009).
[14] Ph. Clément, Approximations by finite element functions using local regularization. *RAIRO Anal. Numer.* **9** (1975) 77–84.
[15] W. Dörfler, M. Rumpf, An adaptive strategy for elliptic problems including *a posteriori* controlled boundary approximation. *Math. Comp.* **67** 1361–1382 (1998).
[16] V.V. Jikov, S.M. Kozlov and O.A. Oleinik, *Homogenization of Differential Operators and Integral Functionals*. Springer, Berlin (1994).
[17] P. Jiranek, Z. Strakos and M. Vohralik, *A posteriori* error estimates including algebraic error: computable upper bounds and stopping criteria for iterative solvers, *SIAM J. Sci. Comput.* **32** (2010) 1567–1590.
[18] P. Neittaanmäki and S.I. Repin, *Reliable Methods for Computer Simulation. Error Control and A Posteriori Estimates*. Elsevier, New York (2004).
[19] S. Repin, *A posteriori* error estimation for nonlinear variational problems by duality theory. *Zapiski Nauch. Semin. (POMI)* **243** (1997) 201–214.
[20] S. Repin, *A posteriori* error estimation for variational problems with uniformly convex functionals. *Math. Comp.* **69** (2000) 481–500.
[21] S. Repin, Two-sided estimates of deviation from exact solutions of uniformly elliptic equations, Proc. of the St. Petersburg Mathematical Society IX, Amer. Math. Soc. Transl. Ser. 2. *Amer. Math. Soc.*, Providence, RI **209** (2003) 143–171.
[22] S. Repin, *A Posteriori Error Estimates For Partial Differential Equations*. Walter de Gruyter, Berlin (2008).
[23] S. Repin and S. Sauter, Functional *a posteriori* estimates for the reaction-diffusion problem. *C. R. Math. Acad. Sci. Paris* **343** (2006) 349–354.
[24] S. Repin and S. Sauter, Computable estimates of the modeling error related to Kirchhoff-Love plate model. *Anal. Appl.* **8** (2010) 1–20.
[25] S. Repin and J. Valdman, Functional *a posteriori* error estimates for problems with nonlinear boundary conditions. *J. Numer. Math.* **16** (2008) 51–81.
[26] S. Repin, S. Sauter and A. Smolianski, *A posteriori* error estimation for the Dirichlet problem with account of the error in the approximation of boundary conditions. *Computing* **70** (2003) 205–233.
[27] S. Repin, S. Sauter and A. Smolianski, Duality based *a posteriori* error estimator for the Dirichlet problem. *Proc. Appl. Math. Mech.* **2** (2003) 513–514.
[28] S. Repin, S. Sauter and A. Smolianski, *A posteriori* estimation of dimension reduction errors for elliptic problems in thin domains. *SIAM J. Numer. Anal.* **42** (2004) 1435–1451.
[29] S. Repin, S. Sauter and A. Smolianski, *A posteriori* control of dimension reduction errors on long domains. *Proc. Appl. Math. Mech.* **4** (2004) 714–715.
[30] S. Repin, S. Sauter and A. Smolianski, *A posteriori* error estimation for the Poisson equation with mixed Dirichlet/Neumann boundary conditions. *J. Comput. Appl. Math.* **164-165** (2004) 601–612.
[31] S. Repin, S. Sauter and A. Smolianski, Two-sided *a posteriori* error estimates for mixed formulations of elliptic problems. *SIAM J. Numer. Anal.* **45** (2007) 928–945.
[32] C. Schwab, *A posteriori* modeling error estimation for hierarchic plate model. *Numer. Math.* **74** (1996) 221–259.
[33] R. Verfürth, A Review of *A Posteriori Error Estimation and Adaptive Mesh-Refinement Techniques*. Wiley-Teubner, Amsterdam (1996).
[34] J. Valdman, Minimization of functional majorant in *a posteriori* error analysis based on H(div) multigrid-preconditioned CG method. *Adv. Numer. Math., Advances Numer. Anal.* (2009) 164519.
[35] M. Vogelius and I. Babuška, On a dimensional reduction method I. The optimal selection of basis functions. *Math. Comput.* **37** (1981) 31–46.